Taper-Integrated Multimode-Interference Based Waveguide Crossing Design

Chyong-Hua Chen and Chia-Hsiang Chiu

***Abstract*— We present a design technique for a compact waveguide crossing by using a 90° multimode-interference (MMI) based waveguide crossing sandwiched by four identical miniaturized tapers where the power of the input guided mode is coupled into even modes of the MMI section at a specific power ratio and with different phases, thereby reducing the dimension of this waveguide crossing with imperceptible loss and crosstalk. Using the finite difference time domain method, we demonstrate that the MMI-based waveguide crossing embedded in short Gaussian tapers has a size 5426 nm × 5426 nm, insertion loss 0.21 dB, and crosstalk −44.4 dB at the wavelength of 1550 nm and broad transmission spectrum ranging from 1500 to 1600 nm.**

***Index Terms*— High index contrast, multimode interference, silicon wire waveguides, waveguide crossings.**

I. Introduction

WAVEGUIDE crossings are essential components for allowing simultaneous processing optical signals from different waveguides within a limited space and the maximization of the number of optical devices in large-scale photonic circuits where optical interconnects are routed in the form of cross-grid arrays [1], [2]. However, as an optical signal propagates through the crossing, the light beam diverges due to the loss of lateral confinement, giving rise to additional insertion loss and crosstalk. In addition, the issues of loss and crosstalk become worse as the optical confinement increases, e.g., silicon wire crossings. A silicon wire crossing with insertion loss exceeding 1 dB and crosstalk approximating −10 dB has been demonstrated numerically and experimentally [3], and this severely restricts the development of compact photonic circuits with a large number of crossings.

To mitigate these problems, various monolithic schemes of waveguide crossings for silicon wire waveguides have been proposed in the literature. A resonator-type crossing is realized to eliminate the crosstalk by introducing a 1-D photonic crystal mirror on each branch of the intersection [4]. However, a Lorentzian transmission response is obtained, which is inappropriate for multiple wavelength transmission. A mode-expander type crossing is designed to suppress the diffraction at the crossing by broadening the waveguide core adiabatically [3], [5], [6]. However, these designs either have a rather large crossing length or require high precision fabrication processes to obtain adequate insertion loss and crosstalk.

On the other hand, multimode-interference (MMI) based crossings are utilized to moderate the diffraction and loss at the crossing by focusing the input beam to a size much smaller than the width of the multimode waveguide at the crossing center [7], [8]. Nevertheless, to re-form a single self-image at the crossing center, the length of the MMI section is required to be twice that of the beat length, at least. Moreover, adiabatically optimized tapers with lengths longer than the beat length are indispensable to minimize the transition losses between the MMI sections and the input/output waveguides. As a consequence, dimensions of the crossings are highly expanded. The footprint of the MMI-based crossing design in [8] is roughly 13 μm × 13 μm, which is more than the square of five times the beat length.

Here, we numerically propose a novel approach to design compact, low-loss, and small-crosstalk 90° MMI-based waveguide crossings integrated with four identical miniaturized tapers. In this miniaturized taper, the power of the input guided wave is converted not only into the fundamental mode of the multimode waveguide but also into higher order modes because of rapid variation in the width of this taper. As a result, the length required to perform the first single self-image in the MMI section is less than the beat length because this taper produces a phase difference between the excited modes. Accordingly, we integrate appropriately designed tapers with a 90° MMI-based waveguide crossing to reduce not only the dimension but also the insertion loss and the crosstalk of this device. By using a 3-D semivectorial finite difference time domain (FDTD) method, numerical studies of waveguide crossings for different taper profiles have been carried out and results show that these crossing structures have lengths less than 2.75 times the beat length, insertion losses less than 0.3 dB, and crosstalks less than −40 dB.

II. Design of Taper-Integrated MMI-Based Waveguide Crossings

A. Device Structure

A single-mode ridge waveguide made of silicon ($n = 3.45$) deposited on a SiO_2 layer ($n = 1.45$) with a width W_g of 500 nm and a height H of 220 nm is designed as the input and the output waveguides. The proposed waveguide crossing consists of a 90° MMI-based waveguide crossing structure connected to the input/output waveguides with four identical tapers, as schematically shown in Fig. 1. The width

Manuscript received April 15, 2010; revised June 8, 2010; accepted June 30, 2010. Date of current version September 8, 2010. This work was supported by the National Science Council of Taiwan under contract NSC 97-2221-E-009-031.

The authors are with the Department of Photonics and Institute of Electro-Optical Engineering, National Chiao Tung University, Hsinchu 30010, Taiwan (e-mail: chyong@mail.nctu.edu.tw; ray_tkd@msn.com).

Color versions of one or more of the figures in this paper are available online at http://ieeexplore.ieee.org.

Digital Object Identifier 10.1109/JQE.2010.2057410

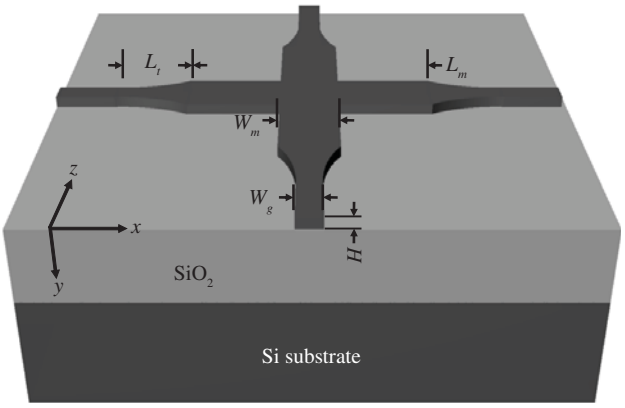

Fig. 1. Schematic structure of the proposed waveguide crossing.

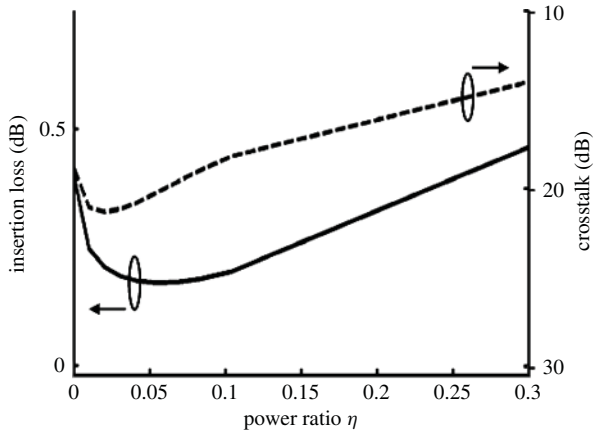

Fig. 2. Calculated insertion loss (solid curve) and crosstalk (dashed curve) of a 90° MMI-based crossing as a function of the power ratio η. The input field is linearly combined by the two lowest order even modes of the multimode waveguide.

W_m of the multimode waveguide is designed to be 1200 nm to support three TE-like modes (i.e., TE_{00}, TE_{01}, and TE_{02} modes) and its length is L_m. The width of the taper varies from W_g to W_m and its length is L_t. These components have the same height as the input/output waveguides, i.e., 220 nm. A 3-D semivectorial FDTD method is used to calculate the performance of this device with the fundamental TE-like mode of the input waveguide ($TE_{00,\text{in}}$ mode) at the wavelength $\lambda_0 = 1550$ nm as the incident wave.

In our design, only the two lowest order even-guided modes of the multimode waveguides are excited inside the MMI section, i.e., the TE_{00} and TE_{02} modes, because of the structure symmetry. The beat length (L_B) between these two modes is given by

$$L_B = \frac{2\pi}{(\beta_{0,0} - \beta_{0,2})} \tag{1}$$

where $\beta_{0,j}$ is the propagation constant of the TE_{0j} mode, $j = 0$ and 2.

The effective refractive indices of the TE_{00} and TE_{02} modes at λ_0 are 2.731 and 2.091, respectively, calculated by 3-D beam propagation method. The corresponding beat length L_B is 2423.6 nm.

B. 90° MMI-Based Crossings at Different Power Ratios

It is known that the scattering loss at the MMI-based crossing is significantly reduced as the beam synthesized from a specific superposition of the guided modes of the multimode waveguide comes to a focus at the crossing center [8], [9]. By using mode propagation analysis [10], the input field $E_{in}(x, y)$ at the junction of the taper and the MMI section linear combination of even guided modes of the multimode waveguide can be written as follows:

$$E_{in}(x, y) = C_{0,0}E_{00}(x, y) + C_{0,2}E_{02}(x, y) \tag{2}$$

where $C_{0,j}$ is the modal coefficient of the modal field distribution $E_{0j}(x, y)$ corresponding to the TE_{0j} mode, $j = 0$ and 2, and calculated by overlap integral.

Here, we investigate the effect of the modal coefficients on the performance of the 90° MMI-based crossings without including the tapers. Let us define a power ratio η as $|C_{0,2}/C_{0,0}|^2$. The modal field composed of a superposition of the TE_{00} and TE_{02} modes at a power ratio of η is incident on the MMI waveguide. Fig. 2 illustrates the calculated loss and crosstalk of a 90° MMI-based crossing with their lengths of $2 \times L_B$ at λ_0 as a function of the power ratio η. We see that $\eta = 0.057$ is found to achieve the minimum loss (~ 0.175 dB). At $\eta < 0.057$, the loss is predominantly attributed to the mode mismatch between the diverged beam after passing through the crossing and the guided modes of the multimode waveguide. On the contrary, as $\eta > 0.057$, a large amount of the TE_{02} mode possessing a wide angular spectrum scatters through the crossing and some of it radiates into the orthogonal MMI sections, resulting in substantial loss and crosstalk.

On examining the modal distribution of the input field at the power ratio = 0.057 shown in Fig. 3, we find that its power distribution fits well with a Gaussian function in the both x and y directions. In comparison with the field distribution of the TE_{00} mode, the horizontal cross section of the input modal field has a much narrower beam width, showing that a focusing beam is obtained at the distance L_B of the MMI section where the first single self-image of the excited field is reproduced.

C. Taper-Integrated MMI Waveguide Lenses

From the previous discussion, we obtain minimal loss and negligible crosstalk of a 90° MMI-based waveguide crossing as a focusing Gaussian field comprised of the TE_{00} and TE_{02} modes at the power ratio of 0.057 is launched onto the multimode waveguide. We can synthesize this field profile by using the MMI lens structure consisting of a multimode waveguide integrated with a miniaturized taper. Here, the studied taper profiles expand in width from an initial value of 500 nm to the final value of 1200 nm and are given as follows:

$$W_t(z) = 500 + 700\left(z/L_{t,0.5}\right)^{0.5} \quad \text{(radical taper)} \tag{3a}$$

$$W_t(z) = 500 + 700\left(z/L_{t,1}\right) \quad \text{(linear taper)} \tag{3b}$$

$$W_t(z) = 500 + 700\left(z/L_{t,2}\right)^2 \quad \text{(quadratic taper)} \tag{3c}$$

$$W_t(z) = 390.44 + 809.56\exp(-2(z - L_{t,g})^2/L_{t,g}^2) \quad \text{(Gaussian taper)} \tag{3d}$$

where $W_t(z)$ is the taper width in nanometers and $L_{t,0.5}$, $L_{t,1}$, $L_{t,2}$, and $L_{t,g}$ are the lengths of the radical, linear, quadratic and Gaussian tapers, respectively.

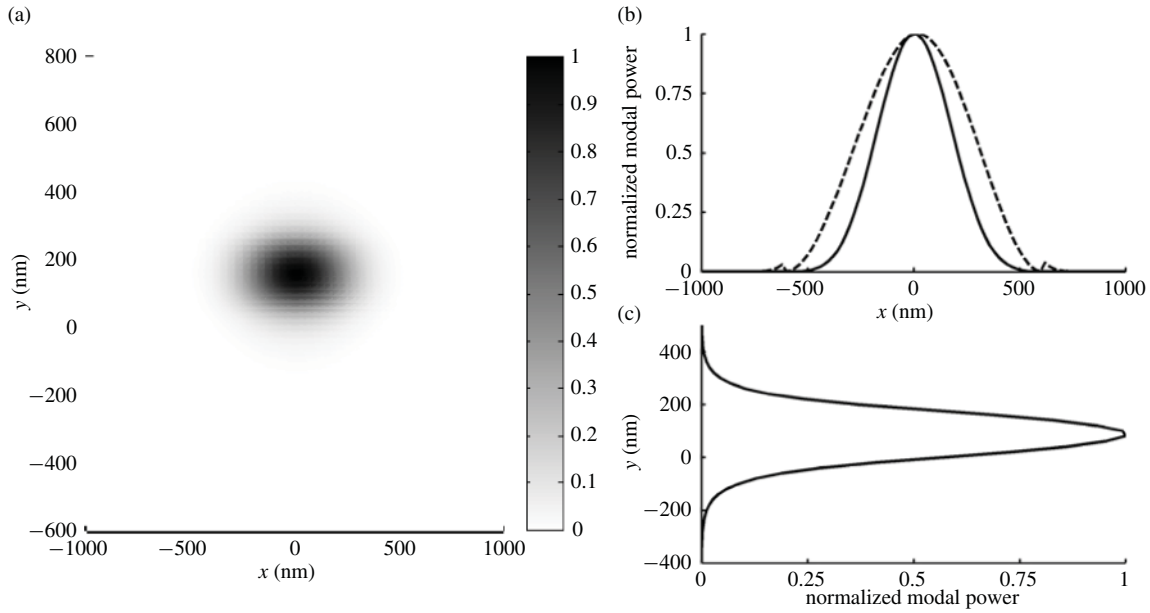

Fig. 3. (a) Power distribution of the modal field combined by the two lowest order even modes at the power ratio of 0.057. (b) Horizontal cross sections at $y = H/2$. (c) Vertical cross sections at $x = 0$ of the combined modal profiles (solid curves) and the TE_{00} mode (dashed curves).

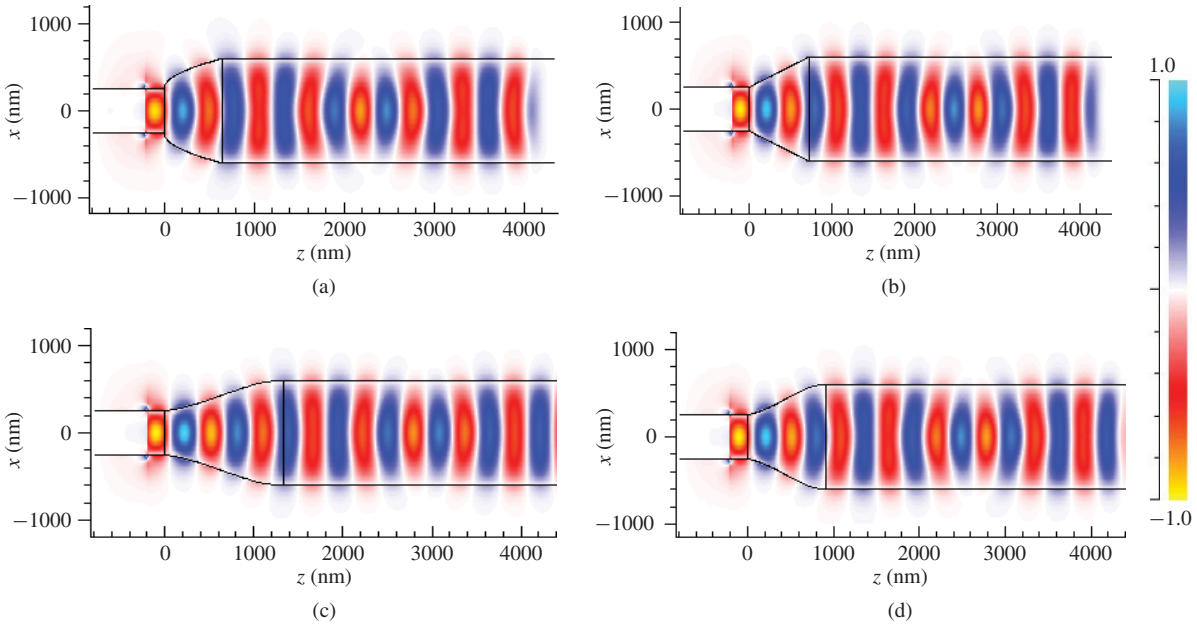

Fig. 4. Evolution of the input guided mode propagation through the MMI lens using (a) radical taper with $L_{t,0.5} = 650$ nm, (b) linear taper with $L_{t,1} = 730$ nm, (c) quadratic taper with $L_{t,2} = 1340$ nm, and (d) Gaussian taper with $L_{t,g} = 920$ nm.

In order to realize $\eta = 0.057$ at λ_0, $L_{t,0.5}$, $L_{t,1}$, $L_{t,2}$, and $L_{t,g}$ are designed to be 650, 730, 1340, and 920 nm, respectively. Fig. 4 shows the simulated propagation behaviors of the $TE_{00,in}$ mode through these taper-integrated MMI lenses. The $TE_{00,in}$ mode diverges along each transverse taper and then converges at some distance L_{eff} of the multimode waveguide where the first smallest beam waist is observed. Here, L_{eff} is called the effective beat length and can be calculated by

$$L_{eff} = \frac{2\pi - \Delta\theta}{(\beta_{0,0} - \beta_{0,2})} \tag{4}$$

where $\Delta\theta$ is the phase difference between $C_{0,0}$ and $C_{0,2}$ at the input face of the multimode waveguide.

From the mode propagation simulations, the phase differences ($\Delta\theta$) obtained for these lenses using the radical, linear, quadratic, and Gaussian tapers are 1.696, 1.201, 1.131, and 1.634 radians, respectively, and thus the respective effective beat lengths L_{eff} are 1769, 1960, 1987, and 1793 nm, all of which less than the beat length. In addition, the corresponding coupling losses of these tapers are 0.081, 0.061, 0.046, and 0.034 dB, demonstrating that these rapidly varying tapers

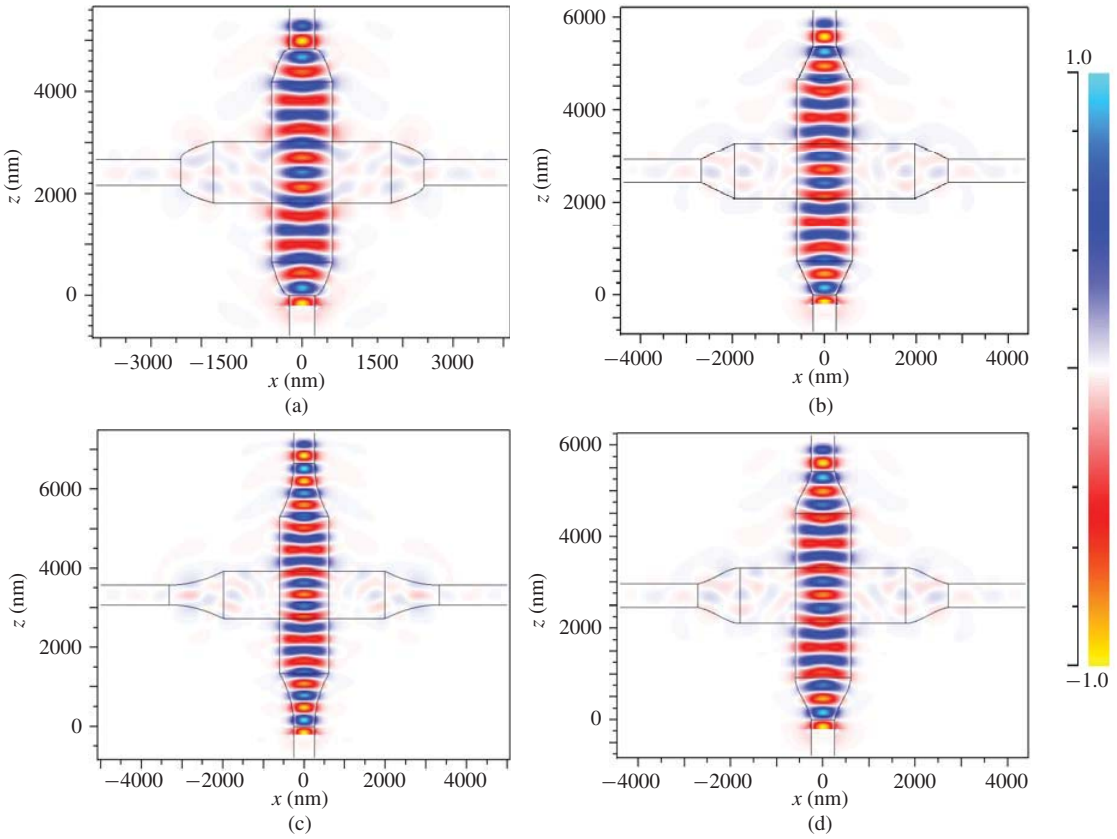

Fig. 5. FDTD simulations of the input guided mode propagation through the 90° MMI-based waveguide crossing embedded in four identical (a) radical tapers with $L_t = 650$ nm and $L_m = 3538$ nm, (b) linear tapers with $L_t = 730$ nm and $L_m = 3920$ nm, (c) quadratic tapers with $L_t = 1340$ nm and $L_m = 3974$ nm, and (d) Gaussian tapers with $L_t = 920$ nm and $L_m = 3586$ nm.

TABLE I
PERFORMANCE OF WAVEGUIDE CROSSINGS WITH DIFFERENT TAPER PROFILES AT λ_0

Taper profile	Taper length L_t (nm)	MMI length L_m (nm)	Crossing dimension (nm × nm)	Insertion loss (dB)	Crosstalk (dB)
Radical	650	3538	4838 × 4838	0.31	−40.02
Linear	730	3920	5380 × 5380	0.24	−42.94
Quadratic	1340	3974	6654 × 6654	0.26	−44.64
Gaussian	920	3586	5426 × 5426	0.21	−44.40

mitigate the transition losses between the input/output and multimode waveguides (∼ 0.2 dB).

D. Taper-Integrated MMI-Based Waveguide Crossings

We use the aforementioned taper-integrated MMI lenses to construct fourfold symmetric waveguide crossings with $L_m = 2 \times L_{eff}$, as depicted in Fig. 1. Fig. 5 illustrates the input guided $TE_{00,in}$ mode propagating through these implemented waveguide crossings integrated with (a) radical, (b) linear, (c) quadratic, and (d) Gaussian tapers, respectively. We see a narrowing of the beam at the center of the crossing and nearly identical wave fronts with a reversal in sign of the phases at the front and back of the crossing in these designs. Furthermore, the propagation behaviors of the beams at the crossings are similar in these examples because the excited fields in the multimode waveguides are composed at the same power ratio.

Table I lists the design parameters and performance of simulated MMI-based crossings at λ_0 using different L_t values and the corresponding optimized L_m values for the crossings using radical, linear, quadratic, and Gaussian tapers. The total lengths of these devices are less than 2.75 times the beat length. The insertion loss of each design is approximately equal to the sum of the losses in a 90° MMI-based crossing and coupling losses caused by the input and output tapers. Besides, the crosstalk in each design is imperceptible, all less than −40 dB. The crosstalks of these designs improve roughly by 20 dB in comparison with that of the design without inserting the tapers shown in Fig. 2, owing to complicated and asymmetric profiles of the scattered waves in the orthogonal waveguides, resulting in significant radiation loss as these fields propagate through the tapers.

Insertion losses and crosstalks of the above-mentioned MMI-based waveguide crossings as a function of wavelength are shown in Fig. 6(a) and (b), respectively. We notice that both the insertion loss and the crosstalk grow with increase of the wavelength in these examples. This is because the coupling

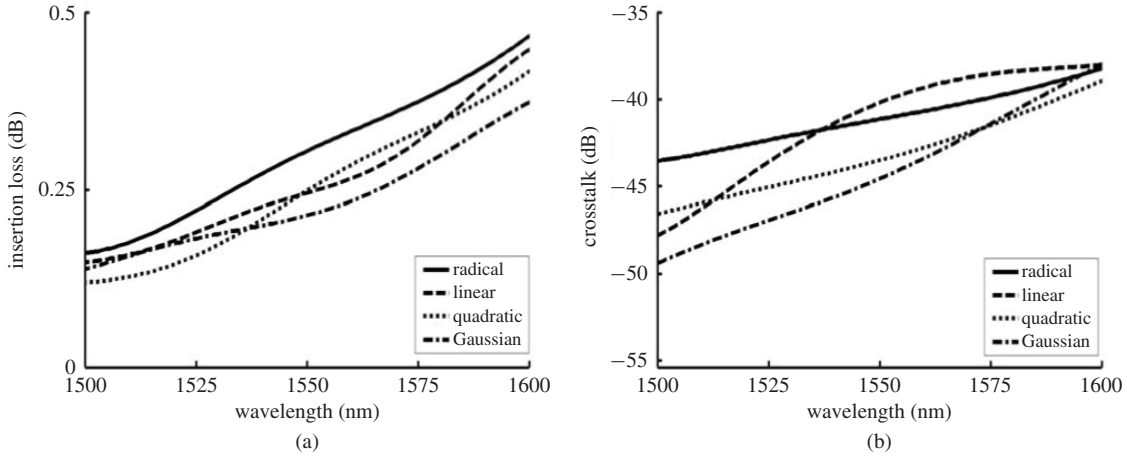

Fig. 6. Wavelength dependence of (a) insertion loss and (b) crosstalk for the MMI-based waveguide crossings by the use of the radical tapers (solid curves), linear tapers (dashed curves), quadratic tapers (dotted curves), and Gaussian tapers (dashed-dotted curves).

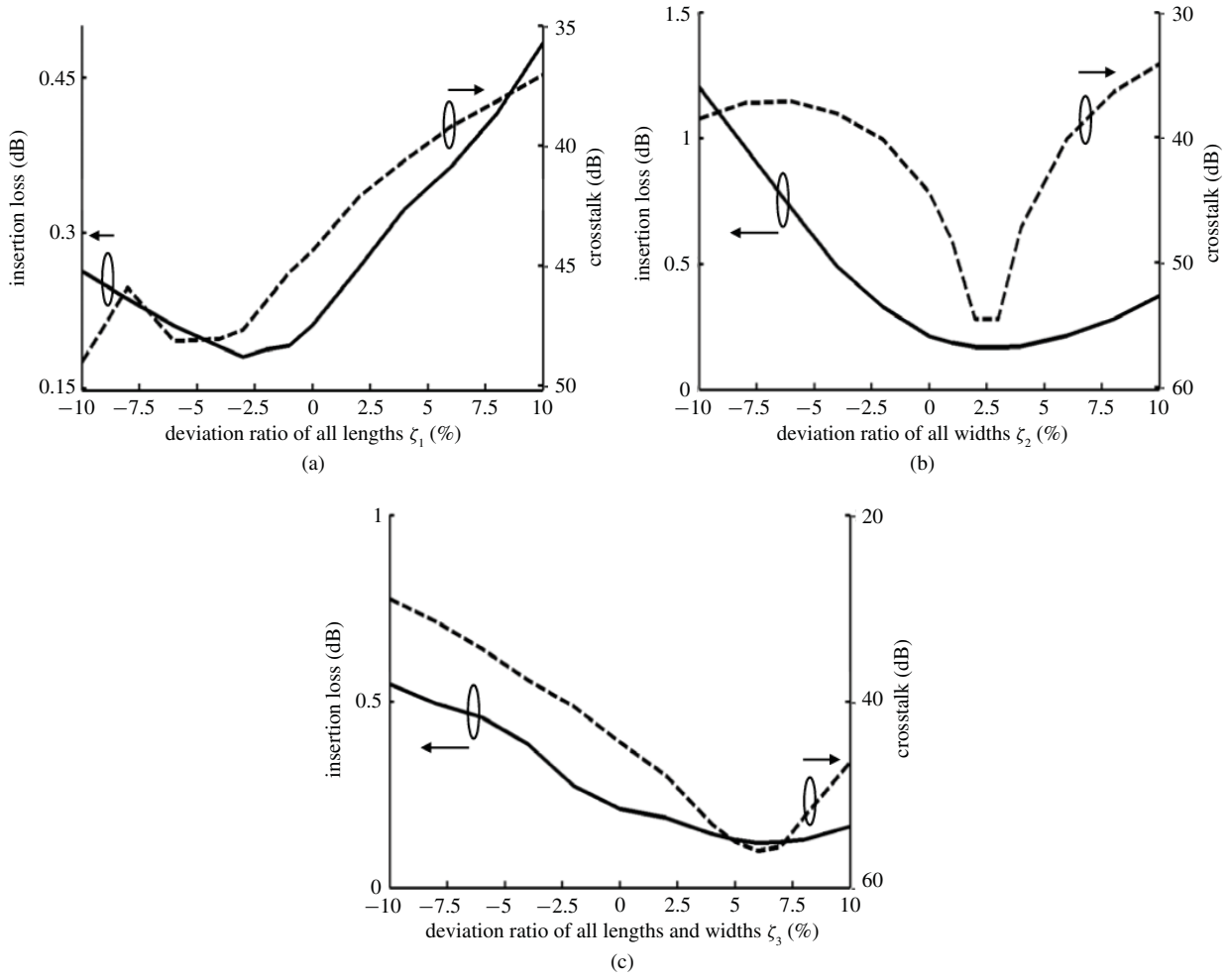

Fig. 7. Insertion loss (solid curves) and crosstalk (dashed curves) vs. deviation ratio of (a) all lengths ζ_1, (b) all widths ζ_2, and (c) all lengths and widths ζ_3 of all waveguides in the Gaussian-taper integrated waveguide crossing structure.

losses of the tapers become higher, the power ratio η becomes larger, and the effective beat length L_{eff} becomes shorter with the increase of the wavelength, the input field is focused in front of the crossing center at longer wavelength, and, as a consequence, the wave is slightly diffracted at the back of the crossing and some of it is scattered into the orthogonal waveguides. Nevertheless, in each design the fluctuation in the insertion loss is less than 0.3 dB and the largest value of the crosstalk is less than −38 dB in the wavelength range 1500–1600 nm. In particular, the crossing design using Gaussian tapers has the smallest variation in the insertion loss, which is roughly 0.24 dB.

E. Sensitivity of the Proposed Crossing Integrated with Gaussian Tapers

In this section, we discuss the possible discrepancy in performance between the ideal design and the fabricated device due to inaccurate lengths and widths of all the waveguides in the aforementioned MMI-based crossing integrated with the Gaussian tapers. First, we consider the effect of the variations in the lengths of all waveguides (i.e., L_t and L_m). Both L_t and L_m are varied by the deviation ratio ζ_1, and the calculated insertion loss and crosstalk as a function of ζ_1 are shown in Fig. 7(a). Because within $\pm 10\%$ variations increasing ζ_1 results in the reduction of η, the increase of coupling losses of these tapers, and the increase of L_{eff}, the insertion loss has a concave structure with the minimum at $\zeta_1 \sim -3\%$ and growing insertion loss and crosstalk are obtained at $\zeta_1 > 0$. The insertion loss and the crosstalk are less than 0.49 and -37 dB, respectively, as ζ_1 is varied within $\pm 10\%$, i.e., the variation in the total length is within $\sim \pm 542$ nm.

Next, we discuss the sensitivity of our design to the width variations (i.e., W_g, W_m, and the taper widths). Fig. 7(b) shows the effect of the deviation ratio ζ_2 of all widths on the insertion loss and the crosstalk. We see small variations in the insertion loss at $0 < \zeta_2 < 10\%$ primarily due to the slight reduction of the coupling losses of these tapers and the loss in the 90° MMI-based crossing. As ζ_2 becomes negative, increasing insertion loss and crosstalk are observed as a result of the increase of L_{eff} with decreasing ζ_2; hence the field is diffracted and scattered at the crossing. The insertion loss and the crosstalk are less than 1.2 and -34 dB, respectively, as all the widths are within $\pm 10\%$ deviations.

The insertion loss and crosstalk with different deviation ratio ζ_3 of the lateral dimensions of all waveguides (i.e., all lengths and widths) are illustrated in Fig. 7(c). The insertion loss has a similar tendency as the width variations except that the values are lower and the minimum shifts to $\zeta_3 \sim 6\%$. Besides, the crosstalk becomes worse at $\zeta_3 < 0$ because the shortened L_m causes the input field to focus before the center of the crossing. The insertion loss and the crosstalk are less than 0.55 and -30 dB, respectively, as ζ_3 fluctuates within $\pm 10\%$. In summary, the performance of the designed crossing is affected by variations in the widths or lengths of all waveguides, especially those of the tapers, with a constant ratio that produces the fluctuations of L_{eff}, η, coupling losses of these tapers, and the loss in the 90° MMI-based crossing. In addition, the insertion loss of our design is more sensitive to variations in widths than to variations in lengths and lateral dimensions of all waveguides.

III. Conclusion

We have presented a new design approach to achieve compact MMI-based waveguide crossings by introducing miniaturized tapers in between the input/output waveguides and a 90° MMI-based waveguide crossing. By this rapidly varying taper, the power of the input guided wave is coupled into both the fundamental modes and the next higher even mode of the multimode waveguide at a specific power ratio, thereby not only diminishing the transition losses between the input/output and multimode waveguides but also reducing the required length of the MMI section for producing the first smallest beam waist at the crossing center. Simulation results show that a 90° MMI-based waveguide crossing integrated with 920-nm long Gaussian tapers has a size of 5426 nm × 5426 nm, insertion loss of 0.21 dB, and crosstalk of -44.4 dB at the wavelength of 1550 nm as well as a broad wavelength transmission spectrum. Losses of this proposed structure are predominately determined by the coupling losses of the short tapers and the loss in the 90° MMI-based crossing, and thus better performance can be achieved either by increasing the widths of the MMI sections or by optimizing these taper structures.

References

[1] L. Pavesi and G. Guillot, *Optical Interconnects: The Silicon Approach*. New York: Springer-Verlag, 2006.

[2] N. Sherwood-Droz, H. Wang, L. Chen, B. Lee, A. Biberman, K. Bergman, and M. Lipson, "Optical 4×4 hitless silicon router for optical networks-on-chip (NoC)," *Opt. Exp.*, vol. 16, no. 23, pp. 15915–15922, Nov. 2008.

[3] T. Fukazawa, T. Hirano, F. Ohno, and T. Baba, "Low loss intersection of Si photonic wire waveguides," *Jpn. J. Appl. Phys.*, vol. 43, no. 2, pp. 646–647, Feb. 2004.

[4] S. G. Johnson, C. Manolatou, S. Fan, P. R. Villeneuve, J. D. Joannopoulos, and H. A. Haus, "Elimination of cross talk in waveguide intersections," *Opt. Lett.*, vol. 23, no. 23, pp. 1855–1857, Dec. 1998.

[5] W. Bogaerts, P. Dumon, D. Thourhout, and R. Baets, "Low-loss, low-cross-talk crossings for silicon-on-insulator nanophotonic waveguides," *Opt. Lett.*, vol. 32, no. 19, pp. 2801–2803, Oct. 2007.

[6] P. Sanchis, P. Villalba, F. Cuesta, A. Håkansson, A. Griol, J. V. Galán, A. Brimont, and J. Martí, "Highly efficient crossing structure for silicon-on-insulator waveguides," *Opt. Lett.*, vol. 34, no. 18, pp. 2760–2762, Sep. 2009.

[7] H. L. Liu, H. Tam, P. K. A. Wai, and E. Pun, "Low-loss waveguide crossing using a multimode interference structure," *Opt. Commun.*, vol. 241, nos. 1–3, pp. 99–104, Nov. 2004.

[8] H. Chen and A. W. Poon, "Low-loss multimode-interference-based crossings for silicon wire waveguides," *IEEE Photon. Technol. Lett.*, vol. 18, no. 21, pp. 2260–2262, Nov. 2006.

[9] H. R. Stuart, "Waveguide lenses with multimode interference for low-loss slab propagation," *Opt. Lett.*, vol. 28, no. 22, pp. 2141–2143, Nov. 2003.

[10] L. Soldano and E. Pennings, "Optical multi-mode interference devices based on self-imaging: Principles and applications," *J. Lightw. Technol.*, vol. 13, no. 4, pp. 615–627, Apr. 1995.

Chyong-Hua Chen received the B.S. and M.S. degrees in electrical engineering from the National Tsing Hua University, Hsinchu, Taiwan, in 1995 and 1997, respectively, and the Ph.D. degree in electrical and computer engineering from the University of California, San Diego, in 2006.

She has been an Assistant Professor in the Department of Photonics and Institute of Electro-Optical Engineering, National Chiao Tung University, Hsinchu, since February 2006. Her current research interests include photonic integrated circuits, photonic crystals, and surface plasmon resonances with applications to optical communication, optical sensing, and optical display systems.

Chia-Hsiang Chiu received the B.S. degree in physics from the National Changhua University of Education, Changhua, Taiwan, in 2008, and the M.S. degree in electrooptical engineering from the National Chiao Tung University, Hsinchu, Taiwan, in 2010.

He is currently with the Department of Photonics and Institute of Electro-Optical Engineering, National Chiao Tung University. His current research interests include integrated photonic circuits, optical interconnects, and optical wavelength-division-multiplexing systems.